Polym. Bull. (2017) 74:75–90
DOI 10.1007/s00289-016-1698-z

ORIGINAL PAPER

A novel biosensor based on electro-co-deposition of sodium alginate-Fe_3O_4-graphene composite on the carbon ionic liquid electrode for the direct electrochemistry and electrocatalysis of myoglobin

Xiuqiong Chen[1] · Huiqiong Yan[1] · Zaifeng Shi[1] · Yuhong Feng[2] · Jiacheng Li[2] · Qiang Lin[1] · Xianghui Wang[1] · Wei Sun[1]

Received: 9 January 2016 / Revised: 27 March 2016 / Accepted: 9 May 2016 /
Published online: 14 May 2016

Abstract A novel biosensor based on electro-co-deposition of myoglobin (Mb), sodium alginate (SA), Fe_3O_4-graphene (Fe_3O_4-GR) composite on the carbon ionic liquid electrode (CILE) was fabricated using Nafion as the film forming material to improve the stability of protein immobilized on the electrode surface, and the modified electrode was abbreviated as Nafion/Mb-SA-Fe_3O_4-GR/CILE. FT-IR and UV–vis absorption spectra suggested that Mb could retain its native structure after being immobilized in the SA-Fe_3O_4-GR composite film. The electrochemical behavior of the modified electrode was studied by cyclic voltammetry, and a pair of symmetric redox peaks appeared in the cyclic voltammograms, indicating that direct electron transfer of Mb was realized on the modified electrode, which was ascribed to the good electrocatalytic capability of Fe_3O_4-GR composite, the good biocompatibility of SA and the synergistic effects of SA and Fe_3O_4-GR composite. The electrochemical parameters of the electron transfer number (n), the charge transfer coefficient (α) and the electron transfer rate constant (k_s) were calculated as 0.982, 0.357 and 0.234 s^{-1}, respectively. The modified electrode exhibited good electrocatalytic ability to the reduction of trichloroacetic acid (TCA) with wide linear range from 1.4 to 119.4 mmol/L, low detection limit as 0.174 mmol/L (3σ), good stability and reproducibility.

X. Chen and H. Yan are co-first authors.

✉ Qiang Lin
linqianggroup@163.com

✉ Wei Sun
sunwei@qust.edu.cn

[1] College of Chemistry and Chemical Engineering, Hainan Normal University, Haikou 571100, Hainan, People's Republic of China

[2] College of Materials and Chemical Engineering, Hainan University, Haikou 570228, People's Republic of China

Keywords Electro-co-deposition · Sodium alginate · Fe_3O_4-graphene composite · Carbon ionic liquid electrode · Direct electrochemistry · Electrocatalysis · Myoglobin

Introduction

The novel electrochemical biosensor belonging to the third generation biosensor is constructed based on the direct electron transfer between redox proteins and the electrode [1], aiming at investigating the redox protein-catalyzed reactions in biological systems and metabolic processes involving redox transformations [2, 3]. Myoglobin (Mb), a kind of important redox proteins, possesses the bioactive heme Fe(III)/Fe(II) redox couple which has commonly been employed to construct electrochemical biosensors. Usually, these electrochemical biosensors possess good electrocatalytic activity to the reduction of trichloroacetic acid (TCA), hydrogen peroxide (H_2O_2), sodium nitrite ($NaNO_2$) [4], etc., which are harmful for human health. However, because of the deeply embedded redox active center in the structure of proteins, the direct electron transfer between the redox proteins and the electrode is hard to be achieved [5, 6]. For this reason, it is necessary to conduct the modification of the substrate electrode by the use of different methods and materials, such as electro-co-deposition [7], sol–gel [8], self-assembly [9], covalent binding [10], and polymers [11, 12], inorganic materials [13, 14], metal oxides nanoparticles [15, 16], etc., to facilitate the electron transfer rate between the active center of proteins with the electrode. For example, Abu-Rabeah et al. [17] created a highly responsive glucose biosensor by covalent attachment of glucose oxidase with alginate-pyrrole matrix, followed by pyrrole polymerization. The resulting amperometric glucose biosensor revealed a faster response time and higher glucose sensitivity than the similar biosensor configuration without the pyrrole polymerization process or with entrapped pyrrole. Ding et al. [18] applied *N*-butylpyridinium hexafluorophosphate, sodium alginate and graphite to construct a novel horseradish peroxidase biosensor for the determination of H_2O_2. The obtained new electrode presented very large current response from electroactive substrates due to its enhanced conductivity and biocompatible interface.

Among the above method, electro-co-deposition technology, as an effective way to immobilize proteins within a biocompatible material and improve the stability of biosensor, has attracted considerable interest in the field of electroanalysis science [19, 20]. Electro-co-deposition process not only provides a simple and convenient technique for the construction of protein electrodes with minimum denaturation and strong adherence to the surface of the substrate electrode in contrast to other procedures, but also makes the biosensor fabrication reproducible and uniform dispersion of the electroactive materials in the resulting biocomposite film [20]. Lopez et al. [21] functionalized chitosan films with alginate and prussian blue by the electro-co-deposition method to enhance the performance of microbial fuel cells. Li et al. [22] fabricated the biosensor through the electro-co-deposition of flower-like, spherical, and convex polyhedron gold nanoparticles on boron-doped diamond surface, respectively, to realize their direct electrochemistry of hemoglobin. Sodium

alginate (SA), an anionic natural polymer with a lot of carboxyl groups, is a biocompatible material for the immobilization of proteins by the electro-co-deposition method [23]. Owing to the carboxyl groups, sodium alginate could form alginate acid gels on the anode as a result of the pH decrease at the anode during the electro-co-deposition process. The electro-co-deposition film poses uniform coatings on the substrate electrode, which could provide proteins suitable microenvironments to retain their native structure and enhance the direct electron transfer rate [18, 24].

Graphene (GR), a two-dimensional monolayer of graphite, has recently received tremendous attention because of its unique properties [25, 26], such as fast electron transportation, high thermal conductivity, excellent mechanical stiffness and good biocompatibility, which exhibits a significant potential for sensor application. In addition, many extraordinary properties of GR could be realized after integrated into the assembly of GR-metal oxides for improving its versatility. It is reported that metal oxides are active and durable electrocatalysts for biosensors [27, 28]. Fe_3O_4 magnetic nanoparticle is a kind of half-metallic metal oxide, possessing appealing magnetic properties, nontoxicity, easy synthesis and electrocatalytic capability [29], which has been widely utilized in the field of electrochemistry. For example, Qu et al. [30] constructed a novel sensor based on Fe_3O_4 nanoparticles-multiwalled carbon nanotubes composite film for the determination of nitrite. Zhang et al. [31] successfully prepared Nafion covered core–shell structured Fe_3O_4@graphene nanospheres modified glassy carbon electrode (GCE) and used it for selective detection dopamine. Kingsley et al. [32] fabricated magnetite (Fe_3O_4) nanoparticles modified carbon paste electrode (Fe_3O_4-CME) to achieve facile electrochemical determination of ascorbic acid (AA) and folic acid (FA) using differential pulse voltammetry.

Carbon ionic liquid electrode (CILE), prepared by simply incorporating the binder and the modifier of ionic liquid into the carbon past electrode, possesses the specific advantages, such as excellent conductivity, high sensitivity, wide electrochemical windows and good anti-fouling ability, which has been proved to be an effective working electrode in the field of electrochemical sensor [33, 34]. In general, electro-co-deposition is performed on the metal electrode, such as the bulk gold electrode, while few work of CILE as the substrate electrode applied in the electro-co-deposition process was reported.

In this study, myoglobin-sodium alginate-Fe_3O_4-graphene (Mb-SA-Fe_3O_4-GR) composite film modified carbon ionic liquid electrode (CILE), abbreviated as Nafion/Mb-SA-Fe_3O_4-GR/CILE, was fabricated by the electro-co-deposition method. Fe_3O_4-GR composite and myoglobin (Mb) were first introduced into the sodium alginate matrix and then electro-co-deposited onto the CILE. The SA-Fe_3O_4-GR composite film could efficiently retain the bioactivity of the entrapped Mb. The direct electrochemistry of Mb was realized with the enhanced electrochemical responses on the modified electrode. Electrocatalytic ability of Nafion/Mb-SA-Fe_3O_4-GR/CILE to the reduction of trichloroacetic acid (TCA) was further investigated.

Experimental sections

Materials

Sodium alginate (SA, $M_W = 430$ kda), liquid paraffin and KCl were purchased from Aladdin Chemical Reagent Co., Ltd., Shanghai, China. Ionic liquid *N*-hexylpyridinium hexafluorophosphate ($HPPF_6$) was purchased from Lanzhou Greenchem, ILS, LICP, CAS, China. Graphite powder (particle size 30 mm) was purchased from Shanghai Colloid Chem. Co., China. Graphene (GR) was purchased from the institute of coal chemistry, Chinese academy of sciences, Taiyuan, China. Myoglobin (Mb, $M_W = 17.8$ kda) and Nafion (5 % ethanol solution) were purchased from Sigma, USA. Trichloroacetic acid (TCA) was purchased from Tianjin Kemiou Chemical Ltd. Co., China. Fe_3O_4 nanoparticles are synthesized by co-precipitating aqueous solutions of $(NH_4)_2Fe(SO_4)_2$ and $FeCl_3$ mixtures in alkaline medium [32]. Fe_3O_4-graphene (Fe_3O_4-GR) composite was prepared by blending Fe_3O_4 nanoparticles with GR by ball-milling method. 0.1 mol/L phosphate buffer solutions (PBS, pH 7.0) were used as the supporting electrolyte. The chemicals were of analytical grade and used without further purification. Doubly distilled water was used as a solvent to prepare all solutions.

Methods

Preparation of CILE

The preparation of CILE was carried out through the following steps. Firstly, 3.2 g of graphite powder, 1.6 g of $HPPF_6$ and 1.0 mL of liquid paraffin were mixed thoroughly in a mortar to form a homogeneous carbon paste. Then, a portion of the carbon paste was filled into one end of a glass tube, and a copper wire was inserted through the opposite end to establish an electrical contact. Finally, the surface of CILE was smoothed on a piece of weighing paper prior to use.

Fabrication and characterization of the modified electrode

Mb-Fe_3O_4-GR composite film was electro-co-deposited on the CILE based on the local formation of alginate acid gels. Firstly, a solution containing 1.6 mg/mL SA, 10.0 mg/mL Mb and 1.25 mg/mL Fe_3O_4-GR composite were mixed homogeneously. The mixed solution was purged with highly purified nitrogen for 30 min prior to experiments. Then the modified electrode was achieved by cycling the potential between -1.1 and $+1.0$ V (vs. SCE) at a scan rate of 100 mV/s for 15 consecutive cycles in the mixed solution with a nitrogen atmosphere maintained during the experiments. Finally, 5.0 μL of 0.5 % Nafion solution was spread evenly onto the surface of the modified electrode after its surface was dry at room temperature. Nafion with excellent film-forming ability could improve the stability of materials immobilized on the electrode surface and prevent the leakage of protein from electrode into the solution. This resultant electrode was abbreviated as Nafion/

Mb-SA-Fe_3O_4-GR/CILE. For comparison, the modified electrodes including Nafion/Mb/CILE, Nafion/Mb-SA/CILE and Nafion/Mb-Fe_3O_4-GR/CILE were prepared by the similar procedure.

The structure of Mb and Mb in SA-Fe_3O_4-GR composite matrix was confirmed by FT-IR and UV–vis spectra, and the morphology of the electrode was observed by scanning electron microscope (SEM). FT-IR spectra of sample were recorded on a Tensor 27 Fourier transform infrared spectrometer (Bruker, Germany). The samples were mixed with KBr and compressed to semitransparent disks for spectroscopic analysis. UV–vis spectroscopic experiments were performed with a mixture solution of certain concentrations of samples. Their absorption spectra were recorded on a Cary 50 probe spectrophotometer (Varian, Australia). The morphology of the sample was recorded with a JSM-7100F scanning electron microscope (Electron, Japan) after gold coating.

Electrochemical measurement of the modified electrode

Electrochemical measurement of cyclic voltammetry was performed with a CHI 750B electrochemical workstation at an ambient temperature. A conventional three-electrode system was used with an Mb modified electrode as working electrode, a platinum wire electrode as auxiliary electrode and a saturated calomel electrode (SCE) as reference electrode. Direct electrochemistry of the modified electrode and electrocatalysis of TCA were performed in a 10 mL electrochemical cell containing 0.1 mol/L phosphate buffer solution and 0.1 mol/L PBS containing various concentrations of TCA, respectively, which were purged with highly purified nitrogen for 30 min prior to experiments with a nitrogen atmosphere maintained during the experiments.

Results and discussion

Fabrication and characterization of the modified electrode

Figure 1 shows the cyclic voltammograms of the electrodeposition of Mb-SA-Fe_3O_4-GR composite film onto the CILE in the mixture solution of 1.6 mg/mL SA, 10.0 mg/mL Mb and 1.25 mg/mL Fe_3O_4-GR composite. The thickness of the resultant Mb-SA-Fe_3O_4-GR composite film was varied in the range of 1.2–2.7 μm obtained from SEM measurements (data not shown). During the electro-co-deposition process, an electrochemical sensing platform was constructed based on the integration of natural polysaccharide alginate, biocompatible Fe_3O_4-GR composite and redox proteins (Mb). Electro-co-deposition of the mixture could uniformly form Mb-SA-Fe_3O_4-GR biocomposite film on the CILE. As the molecular charge and solubility of SA are pH dependent, it becomes ideally suitable material for electro-co-deposition by local formation of alginate acid gels to immobilize proteins and provide them microenvironments to retain their native structure. The proposed mechanism of gel formation is based on the pH decrease at the anode owing to the electrochemical decomposition of water [20, 23].

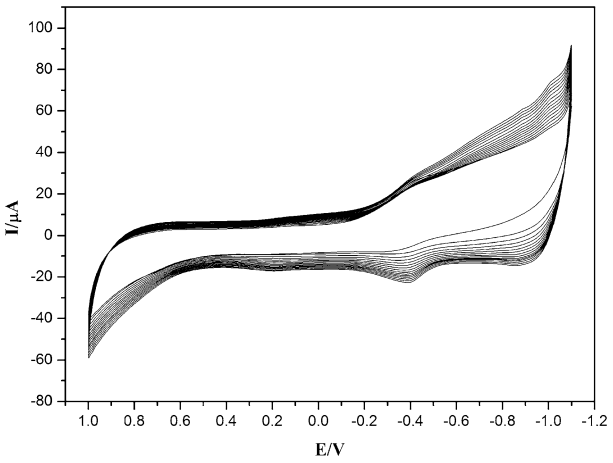

Fig. 1 The cyclic voltammograms of Mb-SA-Fe_3O_4-GR composite progressive course on the CILE between −1.1 and +1.0 V (vs. SCE) at a scan rate of 100 mV/s for 15 consecutive scans

$$H_2O \rightarrow 1/2O_2 + 2H^+ + 2e^- \quad (1)$$

The dissociation of SA results in the formation of anionic A^- species.

$$SA \rightarrow Na^+ + A^- \quad (2)$$

The A^- species would form alginate acid (H-A) gel in the low pH region around the electrode.

$$A^- + H^+ \rightarrow H\text{-}A \quad (3)$$

The resultant composite gel film incorporated with Mb is locally electro-co-deposited on the anode surface (CILE). Then, the coating of Nafion film was to prevent the leakage of Mb out of Mb-SA-Fe_3O_4-GR composite.

The morphology of Fe_3O_4-GR composite and the surface morphologies of SA, Mb and Mb-SA-Fe_3O_4-GR composite electro-co-deposited on the CILE could be observed by SEM. As shown in Fig. 2a, Fe_3O_4-GR composite exhibited small particle shape with the size at the nanoscale. SA was able to generate a uniform film on the CILE (Fig. 2b) attributed to the formation of alginate acid gels, which were induced by the decrease of pH around the electrode during the electro-co-deposition process. In Fig. 2c, single Mb revealed the cluster shape on the CILE because of the small deformation of the molecular structure occurred in the process of drying. The results indicated that the active Mb may easily suffer from denaturation without the protection of the biocompatible materials. Alginate acid gels, as the natural and biocompatible materials, not only played an important role to immobilize proteins but also provided proteins good microenvironments to retain their native structure. From Fig. 2d, Mb-SA-Fe_3O_4-GR composites were uniformly electro-co-deposited on the CILE, implying that electro-co-deposition was a feasible way to fabricate the uniform and stable biosensor.

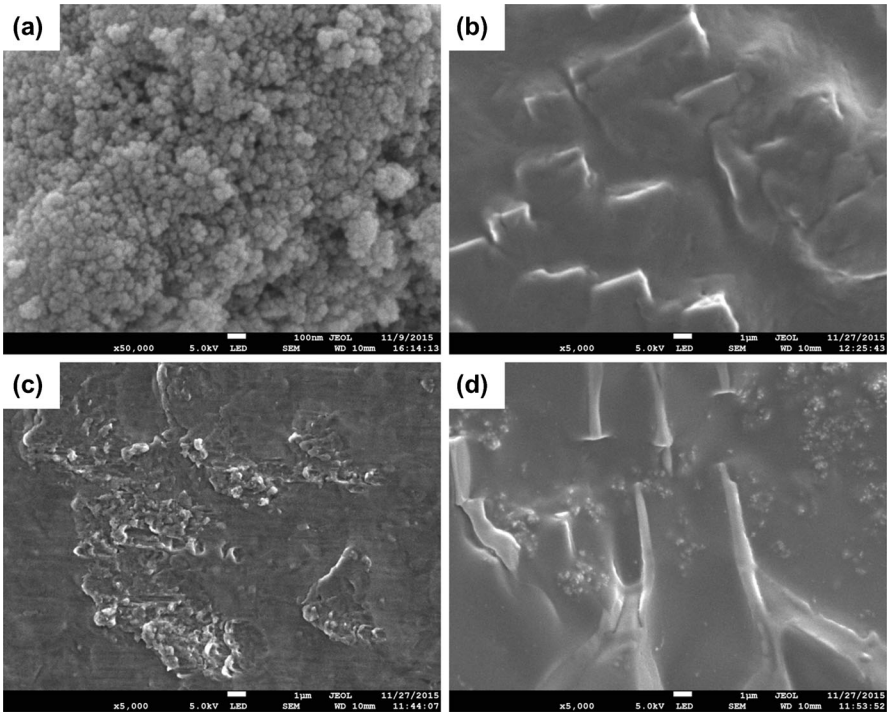

Fig. 2 SEM images of **a** Fe_3O_4-GR composite, **b** SA, **c** Mb and **d** Mb-SA-Fe_3O_4-GR composite

The structure of Mb in Mb-SA-Fe_3O_4-GR composite film could be further investigated by FT-IR and UV–vis absorption spectra. FT-IR spectra of pure Mb and Mb-SA-Fe_3O_4-GR composite film were presented in Fig. 3. The broad and strong peak at 3000–4000 cm^{-1} was assigned to hydroxyl stretching vibrations. The peak of hydroxyl stretching in the spectrum of pure Mb (Fig. 3a) was obviously decreased and broad as compared to that in the spectrum of Mb-SA-Fe_3O_4-GR composite film (Fig. 3b), indicating the presence of the intermolecular hydrogen bonding among Mb-SA-Fe_3O_4-GR composite [35]. Furthermore, Mb-SA-Fe_3O_4-GR composite film exhibited weak characteristic peaks in the curve in contrast to the FT-IR spectrum of pure Mb, owing to the hydrogen bonding or shielding effect stemmed from SA-Fe_3O_4-GR composite. The peaks at 1654.36 and 1542.46 cm^{-1}, respectively, corresponded to amide I and II infrared absorbance peaks of Mb, whose position and shape were similar with that of Mb-SA-Fe_3O_4-GR composite film (1654.03 and 1539.19 cm^{-1}). As the shape and position of the amide I and II infrared absorbance peaks of Mb can provide detailed information on the secondary structure of the polypeptide chain [34], the above results suggested that Mb could keep its native structure after being immobilized in the SA-Fe_3O_4-GR composite film.

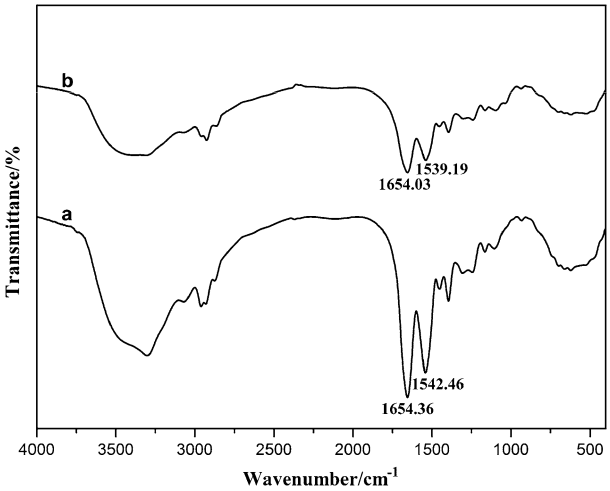

Fig. 3 FT-IR spectra of *a* Mb and *b* Mb-SA-Fe_3O_4-GR composite film

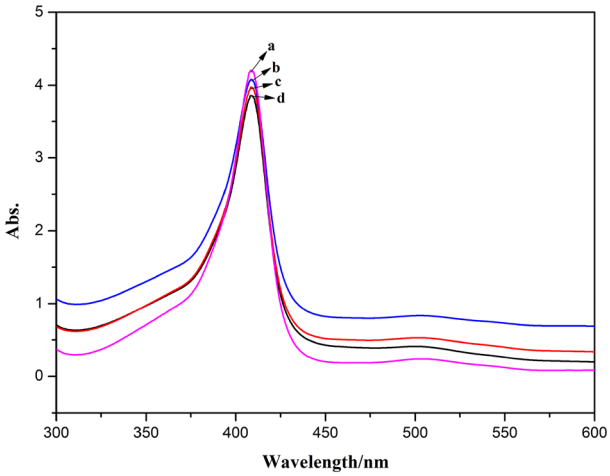

Fig. 4 UV-vis absorption spectra of *a* Mb, *b* Mb-SA, *c* Mb-Fe_3O_4-GR and *d* Mb-SA- Fe_3O_4-GR in pH 7.0 PBS

UV–Vis adsorption spectrum is another way to test the structure change of Mb. As shown in Fig. 4a, Mb showed a characteristic Soret absorption peak at 409.0 nm in pH 7.0 PBS. It is observed that in mixture solutions of Mb-SA (Fig. 4b), Mb-Fe_3O_4-GR (Fig. 4c) and Mb-SA-Fe_3O_4-GR (Fig. 4d), the Soret peaks appeared at the same position (409.0 nm). The results indicated that Mb molecules retained its native structure in the mixture, and SA and Fe_3O_4-GR exhibited good biocompatibility with redox proteins, which were capable of being promising materials in the construction of electrochemical sensors.

Direct electrochemistry of the modified electrode

The electrochemical behavior of the modified electrode was studied by cyclic voltammetry. Figure 5 shows cyclic voltammograms of different modified electrodes in deaerated pH 7.0 PBS at a scan rate of 100 mV/s. There were no obvious redox peaks for Nafion/SA-Fe3O4-GR/CILE, demonstrating no electroactive substances existed on the electrode. Thank to the redox of immobilized Mb, Nafion/Mb-Fe_3O_4-GR/CILE, Nafion/Mb-SA/CILE and Nafion/Mb-SA-Fe_3O_4-GR/CILE exhibited a pair of unsymmetric redox peaks whose reduction peak current was greater than the oxidation peak current, indicating a quasireversible electron transfer process [4]. While the redox peak currents of Nafion/Mb-SA/CILE were bigger than that of Nafion/Mb-Fe_3O_4-GR/CILE, implying that the formation of alginate acid gels by the electro-co-deposition method had more effects on the electron transfer of Mb with CILE than Fe_3O_4-GR composite, though Fe_3O_4-GR possessed good electrocatalytic capability [29]. The good biocompatibility of SA provided redox proteins suitable microenvironment to keep their biological activity, facilitating the electron transfer between redox proteins and the electrode [18]. The synergistic effects of SA and Fe_3O_4-GR composite incorporated in the film accelerated the electron transfer rate, making Nafion/Mb-SA-Fe_3O_4-GR/CILE present biggest redox peak currents among the modified electrodes. From cyclic voltammogram of Nafion/Mb-SA-Fe_3O_4-GR/CILE, the redox peak potentials were recorded with the cathodic peak potential (Epc) as −0.302 V and the anodic peak potential (E_{pa}) as −0.224 V. The formal peak potential ($E^{0'}$) was calculated as −0.263 V (vs. SCE), which was the typical value of the active center of Mb Fe(III)/Fe(II) redox couple [34]. Therefore, the direct electron transfer of Mb was attributed to the heme Fe(III)/Fe(II) redox couple in the Mb molecules and it could be realized on the Nafion/Mb-SA-Fe_3O_4-GR/CILE with fast electron transfer rate.

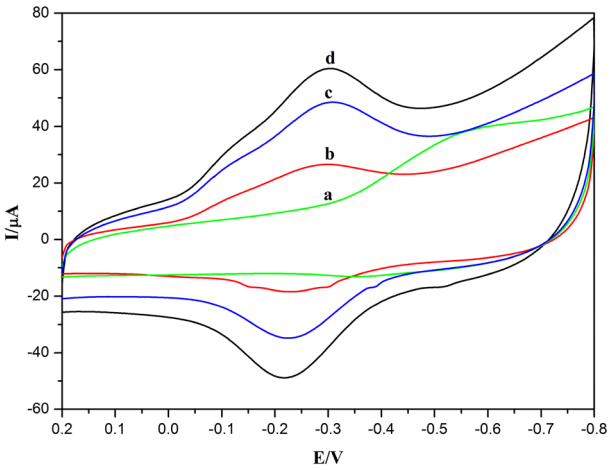

Fig. 5 Cyclic voltammograms of *a* Nafion/SA-Fe_3O_4-GR/CILE, *b* Nafion/Mb-Fe_3O_4-GR/CILE, *c* Nafion/Mb-SA/CILE and *d* Nafion/Mb-SA-Fe_3O_4-GR/CILE in pH 7.0 PBS with the scan rate as 100 mV/s

Figure 6a shows cyclic voltammograms of Nafion/Mb-SA-Fe_3O_4-GR/CILE in pH 7.0 PBS at different scan rates. With the increase of scan rate from 20 to 1000 mV/s, the cyclic voltammograms exhibited a pair of symmetric redox peaks with the nearly equal redox peak currents, which attributed to the reduction and reoxidation of electroactive Mb Fe(III)/Fe(II) redox couple in the composite during the cyclic scanning. As shown in Fig. 6b, both of the redox peak currents increased linearly with scan rate, indicating a surface controlled thin-layer electrochemical reaction. The linear regression equations were calculated as Ipc (μA) = 157.787v (V/s) + 6.454 ($n = 24$, $\gamma = 0.998$) and Ipa (μA) = −165.280v (V/s) − 2.900 ($n = 24$, $\gamma = 0.998$). According to the Faraday's law ($\Gamma^* = Q/nAF$) [6], where F is the Faraday constant, Q is the integration charge of the reduction peak, n is the number of electron transferred, A is the surface area of the electrode. By integration of the cyclic voltammetric curve, the surface concentration (Γ^*) of electroactive Mb can be calculated as 1.83×10^{-9} mol/cm^2, which was much larger than that of monolayer coverage (2.0×10^{-11} mol/cm^2) [36]. The results demonstrated that there were multilayers of Mb existed in the Mb-SA-Fe_3O_4-GR composite film, which was beneficial to exchange electron with the underlying CILE. With the increase of scan rate, the redox peak potentials were also shifted as shown in Fig. 6c, which was a typical quasi-reversible electrode process. The redox peak potentials exhibited linear relationship with natural logarithm of scan rate (ln$v$) in the range from 20 to 1000 mV/s with the equations as E_{pc} (V) = −0.046ln$v$ (V/s)−0.341 ($n = 17$, $\gamma = 0.993$) and E_{pa} (V) = 0.054ln$v$ (V/s)−0.299 ($n = 17$, $\gamma = 0.992$), respectively. So the electrochemical parameters of the electrode reaction can be calculated based on the Laviron's equation (Eqs. 4–6) [37, 38].

$$E_{pa} = E^{0'} + \frac{RT}{(1-\alpha)nF}\ln v \tag{4}$$

$$E_{pc} = E^{0'} - \frac{RT}{\alpha nF}\ln v \tag{5}$$

$$\log k_s = \alpha\log(1-\alpha) + (1-\alpha)\log\alpha - \log\frac{RT}{nFv} - (1-\alpha)\alpha\frac{nF\Delta E_P}{2.3RT} \tag{6}$$

where $E^{0'}$ is the formal potential, α is the electron transfer coefficient, n is the number of electron transferred, v is the scan rate, k_s is the electron transfer rate constant and ΔE_p is the peak-to-peak potential separation. Based on the Eqs. 4–6, the values of the number of electron transferred (n), the electron transfer coefficient (α) and the apparent heterogeneous electron transfer rate constant (k_s) were calculated as 0.982, 0.357 and 0.234 s^{-1}, respectively. The results indicated that about one electron was transferred on the electrode with fast electron transfer rate.

Electrocatalytic ability of Nafion/Mb-SA-Fe_3O_4-GR/CILE to TCA

Since trichloroacetic acid (TCA) is harmful to the environment and human, the accurate determination and reduction of it by the electrochemistry method has a great significance to the protection of environment and the reduction of the health risks.

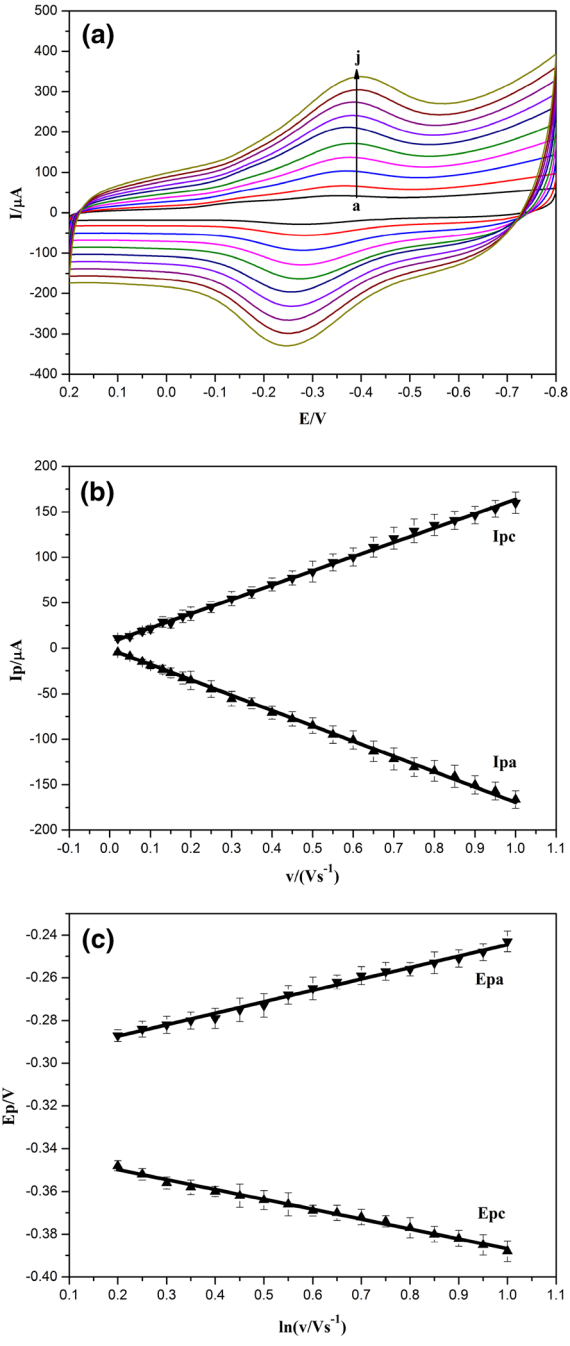

Fig. 6 **a** Cyclic voltammograms of Nafion/Mb-SA-Fe_3O_4-GR/CILE in pH 7.0 PBS at different scan rates (from *a* to *j* are 80, 150, 250, 350, 450, 550, 650, 750, 850, 950 mV/s, respectively); **b** linear relationship of the cathodic **a** and anodic **b** peak current (Ip) versus scan rate (v); **c** linear relationship of the anodic **a** and cathodic **b** peak potential versus ln*v* (*error bars* represent the standard deviation of three replicates)

And the redox proteins usually have good electrocatalytic activity towards TCA [6]. Therefore, this work aimed at studying the electrocatalytic activity to the reduction of TCA. The electrocatalytic activity of Nafion/Mb-SA-Fe_3O_4-GR/CILE to TCA was further investigated. Figure 7 shows the cyclic voltammograms of the Nafion/Mb-SA-Fe_3O_4/CILE in pH 7.0 buffer containing different concentrations of TCA. With the addition of TCA, the reduction peak currents appeared at −0.286 V (vs. SCE) and −0.497 V (vs. SCE) gradually increased, accompanying with the disappearance of the oxidation peak current, which demonstrated the typical characteristic of the electrocatalytic reaction. These two peaks were, respectively, attributed to the electrocatalytic reduction of Mb in the modified electrode for TCA and the formation of a highly reduced form of Mb, which might dechlorinate di- and mono- chloroacetic acid after the dechlorination of TCA with Mb Fe(II) [6]. So the reaction mechanism of electrocatalysis could be described with the following equations (Eqs. 7–11), which included the reduction of Mb Fe(III) to Mb Fe(II), the reduction of TCA with Mb Fe(II), the reduction of Mb Fe(II) to Mb Fe(I), the reduction of di- and mono-chloroacetic acid with Mb Fe(II) and the reoxidation of Mb Fe(I) [6].

$$\text{Mb Fe (III)} + \text{e} \rightarrow \text{Mb Fe (II)} \tag{7}$$

$$2\text{Mb Fe (II)} + \text{Cl}_3\text{CCOOH} + \text{H}^+ \rightarrow 2\text{Mb Fe (III)} + \text{Cl}_2\text{CHCOOH} + \text{Cl}^- \tag{8}$$

$$\text{Mb Fe (II)} + \text{e} \rightarrow \text{Mb Fe (I)} \tag{9}$$

$$2\text{Mb Fe (I)} + \text{Cl}_2\text{CHCOOH} + \text{H}^+ \rightarrow 2\text{Mb Fe (II)} + \text{ClCH}_2\text{COOH} + \text{Cl}^- \tag{10}$$

$$2\text{Mb Fe (I)} + \text{ClCH}_2\text{COOH} + \text{H}^+ \rightarrow 2\text{Mb Fe (II)} + \text{CH}_3\text{COOH} + \text{Cl}^- \tag{11}$$

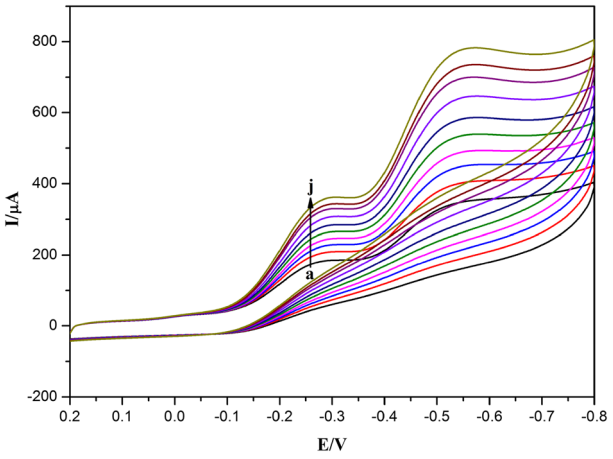

Fig. 7 Cyclic voltammograms of Nafion/Mb-SA-Fe_3O_4-GR/CILE in pH 7.0 PBS containing 1.4, 3.4, 5.4, 10.4, 16.4, 33.4, 53.4, 72.4, 100.4, 130.4 mmol/L TCA (*curves a–j*), respectively, with the scan rate as 100 mV/s

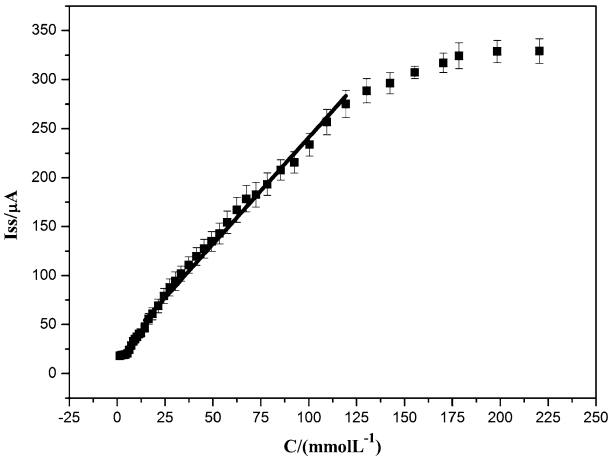

Fig. 8 Linear relationship of catalytic reduction peak currents and the TCA concentration (*error bars* represent the standard deviation of three replicates)

As shown in Fig. 8, there was a good linear relation between the catalytic reduction peak current and the TCA concentration in the range from 1.4 to 119.4 mmol/L with the linear regression equation as I_{ss} (μA) = 2.182C (mmol/L) + 21.171 ($n = 26$, $\gamma = 0.982$). The detection limit was calculated as 0.174 mmol/L (3σ), which was lower than that of the previous reported results of 0.200 mmol/L on Nafion/Mb/Co/CILE [7] and 0.613 mmol/L on CTS/ZnWO4-Hb/CILE [39]. As the TCA concentration exceeded 119.4 mmol/L, the catalytic reduction peak currents began to level off and reached a plateau, implying a Michaelis–Menten kinetic process. The apparent Michaelis–Menten constant (K_M^{app}), being indicative of the enzyme-substrate kinetics, could be calculated by the Lineweaver–Burk equation (Eq. 12) [40].

$$\frac{1}{I_{SS}} = \frac{1}{I_{max}} + \frac{K_M^{app}}{I_{max}C} \tag{12}$$

where I_{ss} is the steady-state current, I_{max} is the maximum current under saturated substrate condition, and C is the bulk concentration of the substrate. Based on Eq. 12, the K_M^{app} value was calculated as 29.1 mmol/L, which is smaller than the reported values of 90.8 mmol/L on Nafion-BMIMPF$_6$/Mb/CILE [41] and 177.0 mmol/L on Mb-agarose/GCE [36]. The results revealed that the immobilized Mb in SA-Fe_3O_4-GR composite film exhibited high affinity to TCA with good enzymatic activity.

Stability and reproducibility of Nafion/Mb-SA-Fe_3O_4-GR/CILE

The stability and reproducibility of Nafion/Mb-SA-Fe_3O_4-GR/CILE was evaluated by measuring the cyclic voltammetric peak currents of Mb. The modified electrode could retain the direct electrochemistry of the immobilized Mb at constant current

values upon the continuous cyclic voltammetric sweep for 120 cycles. When stored at 4 °C for over 2 weeks, the Nafion/Mb-SA-Fe_3O_4-GR/CILE retained 97.2 % of the initial current response. After 1 month, the peak current response decreased about 7.5 %. The good long-term stability can be attributed to the good biocompatibility of SA-Fe_3O_4-GR composites, which can provide a favorable microenvironment for Mb to retain its bioactivity. With the independent preparation of 10 modified electrodes by the same procedure for the electrochemical detection of 10.0 mmol/L TCA, the results showed acceptable reproducibility with the relative standard deviations of 6.1 %. On the basis of above results, Nafion/Mb-SA-Fe_3O_4-GR/CILE fabricated by the electro-co-deposition method exhibited good stability and reproducibility.

Conclusion

In this work, the active Mb and biocompatible SA-Fe_3O_4-GR composite were successfully electro-co-deposited onto the surface of CILE to fabricate Nafion/Mb-SA-Fe_3O_4-GR/CILE. Owing to the good biocompatibility of SA, the local formation of alginate acid gels by the electro-co-deposition method provided Mb suitable microenvironment to keep its biological activity. Direct electron transfer of Mb was realized on the modified electrode, which was ascribed to the good electrocatalytic capability of Fe_3O_4-GR composite, the good biocompatibility of SA and the synergistic effects of SA and Fe_3O_4-GR composite. The constructed third-generation biosensor displayed wide linear range from 1.4 to 119.4 mmol/L, low detection limit as 0.174 mmol/L (3σ), good stability and reproducibility for the reduction of TCA, which would be capable of being a potential biosensing platform in the electroanalysis and electrocatalysis.

Acknowledgments We gratefully thank the financial support form the National Natural Science Foundation of China (21366010, 21566009) and Key Projects in the Hainan provincial Science & Technology Program (ZDXM2014037).

References

1. Xu J, Liu CH, Teng YL (2010) Direct electrochemistry and electrocatalysis of hydrogen peroxide using hemoglobin immobilized in hollow zirconium dioxide spheres and sodium alginate films. Microchim Acta 169:181–186
2. Pulcu GS, Elmore BL, Arciero DM, Hooper AB, Elliott SJ (2007) Direct electrochemistry of tetraheme cytochrome c554 from nitrosomonas europaea: redox cooperativity and gating. J Am Chem Soc 129(7):1838–1839
3. Kang XH, Wang J, Wu H, Aksay IA, Liu J, Lin YH (2009) Glucose oxidase-graphene-chitosan modified electrode for direct electrochemistry and glucose sensing. Biosens Bioelectron 25:901–905
4. Sun W, Cao LL, Deng Y, Gong SX, Shi F, Li GN, Sun ZF (2013) Direct electrochemistry with enhanced electrocatalytic activity of hemoglobin in hybrid modified electrodes composed of graphene and multi-walled carbon nanotubes. Anal Chim Acta 781:41–47
5. Andreu R, Ferapontova EE, Gorton L, Calvente JJ (2007) Direct electron transfer kinetics in horseradish peroxidase electrocatalysis. J Phys Chem B 111(2):469–477

6. Sun W, Guo YQ, Ju XM, Zhang YY, Wang XZ, Sun ZF (2013) Direct electrochemistry of hemoglobin on graphene and titanium dioxide nanorods composite modified electrode and its electrocatalysis. Biosens Bioelectron 42:207–213
7. Sun W, Li XQ, Qin P, Jiao K (2009) Electrodeposition of Co nanoparticles on the carbon ionic liquid electrode as a platform for myoglobin electrochemical biosensor. J Phys Chem C 113(26):11294–11300
8. Wang BQ, Zhang JZ, Cheng GJ, Dong SJ (2000) Amperometric enzyme electrode for the determination of hydrogen peroxide based on sol-gel/hydrogel composite film. Anal Chim Acta 407(1–2):111–118
9. Wang G, Lu H, Hu N (2007) Electrochemically and catalytically active layer-by-layer films of myoglobin with zirconia formed by vapor-surface sol-gel deposition. J Electroanal Chem 599(1):91–99
10. Doretti L, Ferrara D, Lora S, Palma G (1999) Amperometric biosensor involving covalent immobilization of choline oxidase and butyrylcholinesterase on a methacrylate-vinylene carbonate copolymer. Biotechnol Appl Biochem 29(1):67–72
11. Lu Q, Hu SS (2006) Studies on direct electron transfer and biocatalytic properties of hemoglobin in polytetrafluoroethylene film. Chem Phys Lett 424(1–3):167–171
12. Zhao HY, Zheng W, Meng ZX, Zhou HM, Xu XX, Li Z, Zheng YF (2009) Bioelectrochemistry of hemoglobin immobilized on a sodium alginate-multiwall carbon nanotubes composite film. Biosens Bioelectron 24(8):2352–2357
13. Zhao G, Feng JJ, Xu JJ, Chen HY (2005) Direct electrochemistry and electrocatalysis of heme proteins immobilized on self assembled ZrO_2 film. Electrochem Commun 7(7):724–729
14. Topoglidis E, Astuti Y, Duriaux F, Grätzel M, Durrant JR (2003) Direct electrochemistry and nitric oxide interaction of heme proteins adsorbed on nanocrystalline tin oxide electrodes. Langmuir 19(17):6894–6900
15. Pandey P, Datta M, Malhotra BD (2008) Prospects of nanomaterials in biosensors. Anal Lett 41(2):159–209
16. Zhou H, Gan X, Wang J, Zhu XL, Li GX (2005) Hemoglobin-based hydrogen peroxide biosensor tuned by the photovoltaic effect of nano titanium dioxide. Anal Chem 77(18):6102–6104
17. Abu-Rabeah K, Marks RS (2009) Impedance study of the hybrid molecule alginate-pyrrole: demonstration as host matrix for the construction of a highly sensitive amperometric glucose biosensor. Sensor Actuator B Chem 136:516–522
18. Ding CF, Zhang ML, Zhao F, Zhang SS (2008) Disposable biosensor and biocatalysis of horseradish peroxidase based on sodium alginate film and room temperature ionic liquid. Anal Biochem 378:32–37
19. Mittal A, Khurana S, Singh H, Kamboj RC (2005) Characterization of dipeptidylpeptidase IV (DPP IV) immobilized in Ca alginate beads. Enzyme Microb Technol 37(3):318–323
20. Liu CH, Guo XL, Cui HT, Yuan R (2009) An amperometric biosensor fabricated from electro-co-deposition of sodium alginate and horseradish peroxidase. J Mol Catal B Enzym 60:151–156
21. Navanietha KR, Karthikeyan R, Sheela B, Saravanan C, Parimal P (2013) Functionalization of electrochemically deposited chitosan films with alginate and Prussian blue for enhanced performance of microbial fuel cells. Electrochim Acta 112:465–472
22. Li MF, Zhao GH, Geng R, Hu HK (2009) Facile electrocatalytic redox of hemoglobin by flower-like gold nanoparticles on boron-doped diamond surface. Bioelectrochemistry 74(1):217–221
23. Cheong M, Zhitomirsky I (2008) Electrodeposition of alginic acid and composite films. Colloid Surf A 328:73–78
24. Freeman I, Kedem A, Cohen S (2008) The effect of sulfation of alginate hydrogels on the specific binding and controlled release of heparin-binding proteins. Biomaterials 29(22):3260–3268
25. Novoselov KS, Geim AK, Morozov SV, Jiang D, Zhang Y, Dubonos SV, Grigorieva IV, Firsov AA (2004) Electric field effect in atomically thin carbon films. Science 306:666–669
26. Joshi RK, Carbone P, Wang FC, Kravets VG, Su Y, Grigorieva IV, Wu HA, Geim AK, Nair RR (2014) Precise and ultrafast molecular sieving through grapheme oxide membranes. Science 343(6172):752–754
27. Yang J, Strickler JR, Gunasekaran S (2012) Indium tin oxide-coated glass modified with reduced graphene oxide sheets and gold nanoparticles as disposable working electrodes for dopamine sensing in meat samples. Nanoscale 4:4594–4602
28. Meisl JR, Qu ZW, Zhu H, Kroes GJ, Norskov JK (2007) Electrolysis of water on oxide surfaces. J Electroanal Chem 607:83–89

29. He Z, Gudavarthy RV, Koza JA, Switzer JA (2011) Room-temperature electrochemical reduction of epitaxial magnetite films to epitaxial iron films. J Am Chem Soc 133:12358–12361
30. Qu JY, Dong Y, Wang Y, Xing HH (2015) A novel sensor based on Fe_3O_4 nanoparticles–multiwalled carbon nanotubes composite film for determination of nitrite. Sens BioSens Res 3:74–78
31. Zhang WX, Zheng JZ, Shi JG, Lin ZQ, Huang QT, Zhang HQ, Wei C, Chen JH, Hu SR, Hao AY (2015) Nafion covered core–shell structured Fe_3O_4@graphene nanospheres modified electrode for highly selective detection of dopamine. Anal Chim Acta 853:285–290
32. Kingsley MP, Desai PB, Srivastava AK (2015) Simultaneous electro-catalytic oxidative determination of ascorbic acid and folic acid using Fe_3O_4 nanoparticles modified carbon paste electrode. J Electroanal Chem 741:71–79
33. Opallo M, Lesniewski A (2011) A review on electrodes modified with ionic liquids. J Electroanal Chem 656:2–16
34. Wang XF, You Z, Sha HL, Gong SX, Niu QJ, Sun W (2014) Direct electrochemistry and electrocatalysis of myoglobin using an ionic liquid-modified carbon paste electrode coated with Co_3O_4 nanorods and gold nanoparticles. Microchim Acta 181:767–774
35. Yan HQ, Chen XQ, Li JC, Feng YH, Shi ZF, Wang XH, Lin Q (2016) Synthesis of alginate derivative via the Ugi reaction and its characterization. Carbohydr Polym 136:757–763
36. Wang SF, Chen T, Zhang ZL, Shen XC, Lu ZX, Pang DW, Wong KY (2005) Direct electrochemistry and electrocatalysis of heme proteins entrapped in agarose hydrogel films in room-temperature ionic liquids. Langmuir 21(20):9260–9266
37. Laviron E (1974) Adsorption, autoinhibition and autocatalysis in polarography and in linear potential sweep voltammetry. J Electroanal Chem 52(3):355–393
38. Laviron E (1979) General expression of the linear potential sweep voltammogram in the case of diffusion less electrochemical systems. J Electroanal Chem 101(1):19–28
39. Ruan CX, Sun ZL, Liu J, Lou J, Gao W, Sun W, Xiao YS (2012) Direct electrochemistry of hemoglobin on an ionic liquid carbon electrode modified with zinc tungstate nanorods. Microchim Acta 177:457–463
40. Kamin RA, Wilson GS (1980) Rotating ring-disk enzyme electrode for biocatalysis kinetic studies and characterization of the immobilized enzyme layer. Anal Chem 52(8):1198–1205
41. Sun W, Li XQ, Jiao K (2009) Direct electrochemistry of myoglobin in a nafion-ionic liquid composite film modified carbon ionic liquid electrode. Electroanalysis 21:959–964